

Contact angle influence on the pull-in voltage of microswitches in the presence of capillary and quantum vacuum effects

George Palasantzas^{a)}

Zernike Institute for Advanced Materials, University of Groningen, Nijenborgh 4, 9747 AG Groningen, The Netherlands

(Received 29 August 2006; accepted 24 December 2006; published online 8 March 2007)

Capillary condensation between the electrodes of microswitches influences the effective pull-in voltage in a manner that depends on the contact angle of the capillary meniscus and the presence of plate surface roughness. Indeed, surface roughening is shown to have a stronger influence on the pull-in potential for relatively small contact angles with respect to that of a flat surface when capillary condensation takes place. For long wavelength roughness ratios $w/\xi \ll 1$ with w the rms roughness amplitude and ξ the in-plane correlation length, the pull-in voltage increases with increasing theoretical contact angle θ_0 for flat surfaces. With decreasing correlation length ξ (increasing roughness), the pull-in potential decreases faster for smaller contact angles θ_0 . In addition, with decreasing roughness exponent H ($0 < H < 1$), which characterizes short wavelength roughness fluctuation at short length scales ($< \xi$), the pull-in potential shows a steeper decrease with decreasing correlation length ξ . Finally, with increasing relative humidity, the sensitivity of the pull-in voltage at small correlation lengths attenuates significantly with increasing contact angle θ_0 .

© 2007 American Institute of Physics. [DOI: 10.1063/1.2472651]

I. INTRODUCTION

The architecture of a diverse variety of microelectromechanical systems/nanoelectromechanical systems (MEMSs/NEMSs) requires the use of microswitches as an essential operation component.¹⁻¹⁴ A typical microswitch is constructed from two conducting electrodes, where one electrode is usually able to move but still remains suspended by a mechanical spring. By applying a voltage difference between the two electrodes, the mobile electrode moves towards the ground electrode due to the electrostatic force. However, at a certain voltage the mobile electrode becomes unstable and collapses or pulls in onto the fixed ground electrode.^{3,4} Besides, pull-in instabilities problems, residual plate stress, and fringing fields influence the operation and failure of microswitches and should be carefully taken into consideration.^{5,6}

Furthermore, when the proximity between the plates of switches becomes of the order of nanometers up to a few microns, a regime is entered where forces that are quantum mechanical in nature, namely, van der Waals (vdW) and Casimir forces, become operative.¹⁵⁻¹⁸ The latter may also be responsible for stiction by causing mechanical elements in close proximity to adhere together, and therefore change the actuation dynamics of switches.⁹ In fact, the Casimir force has been considered to be an exotic quantum phenomenon that results from the perturbation of zero point vacuum fluctuations by the presence of conducting plates.¹⁵⁻¹⁸ Because of its relatively short range (dominant over vdW at separations > 50 nm), it is now starting to attract technological importance for the design and operation of MEMSs/NEMSs.⁹⁻¹³ Recent studies for switches with rough plates have shown that random self-affine roughness, which

often occurs during nonequilibrium film deposition, strongly influences pull-in parameters and phase maps of microswitches in the presence of electrostatic, Casimir, and capillary forces.^{18,19}

Furthermore, MEMSs/NEMSs are fabricated on silicon substrates by deposition and selective etching of multiple layers of structural and sacrificial films.¹⁴ If the resulting surface is hydrophilic, a capillary force develops when the microstructures are pulled out of water or when two surfaces approach each other in humid environments causing adhesion between components. Drying techniques can eliminate release-related adhesion, but they cannot prevent the in-use adhesion where liquids condense from vapor into small cracks and pores in a phenomenon known as capillary condensation.^{14,16} Recently, we studied the influence of capillary forces in combination with electrostatic and quantum vacuum generated forces on the pull-in voltage of microswitches having self-affine rough surfaces.¹⁹ It was shown that the attractive capillary force decreases more the effective electrostatic pull-in voltage when the plate surfaces are rougher. The latter corresponds to smaller roughness exponents H ($0 < H < 1$, which characterize short wavelength roughness) and/or larger long wavelength roughness ratios w/ξ with w the root-mean-square (rms) roughness amplitude and ξ the in-plane correlation length.¹⁹

Therefore, since capillary forces can strongly influence the operation of microswitches, the influence of the capillary meniscus contact angle on the pull-in potential will be further investigated. Indeed, up to now we have not presented any detailed investigation of the influence of the contact angle on pull-in characteristics for rough plate surfaces. This will be the focus in the present work where the elastic restoring force of the moving switch plate will be counterbalanced by capillary, Casimir, and electrostatic forces.

^{a)}Electronic mail: g.palasantzas@rug.nl

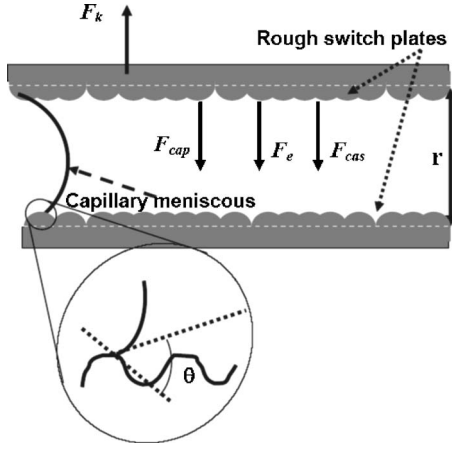


FIG. 1. (Color online) Schematic of parallel plate switch with meniscus formation that exerts the additional capillary force.

II. PULL-IN VOLTAGE OF MICROSWITCHES WITH PARALLEL ROUGH PLATES

We consider a parallel plate configuration where the electrostatic, Casimir, and capillary forces (denoted, respectively, as F_e , F_{Cas} , and F_{cap}) are pulling the plates together and opposing the elastic restoring force F_k (Fig. 1). The initial plate average distance is d , the average flat surface plate area is A_f , the plate spring constant is k and its mass m , the applied voltage in between the plates is V , and the electrical permittivity of the condensed liquid is ϵ . We also assume the same roughness for both plates, which is characterized by single valued random roughness fluctuations $h(R)$ of the in-plane position $R=(x, y)$.

If we consider the second law of Newton to describe the plate motion, $m(d^2r/dt^2)=|F_k|-|F_e|-|F_{Cas}|-|F_{cap}|$, and assume the conditions $|F_k|-|F_e|-|F_{Cas}|-|F_{cap}|=0$ and $d(|F_k|-|F_e|-|F_{Cas}|-|F_{cap}|)/du=0$ (and setting $u=r/d$ and $0 < u < 1$), we obtain the pull-in potential V_{PI} ,^{19,20}

$$\frac{V_{PI}}{V_0} = \left[2u^2 \left(\int_0^{+\infty} e^{-x} \sqrt{1+\rho^2 x} dx \right)^{-1} \left(1-u + \frac{W}{\dot{W}} \right) \left(1 + \frac{2}{u} \frac{W}{\dot{W}} \right)^{-1} - \frac{8\gamma R_{Kel}}{\epsilon V_0^2} \cos^2(\theta) \right]^{1/2}, \quad (1)$$

with $W(u)=u^{-4}[1+(2C_r/d)u]F^T(T, du)$, $\dot{W}=dW/du$, $V_0=\sqrt{kd^3/\epsilon A_f}$, and $\rho=\sqrt{\langle |\nabla h|^2 \rangle}$ the average local surface slope.²¹ We also have the definitions^{19,22}

$$C_r = 0.4492 \int_{Q_r}^{Q_c} q \langle |h(q)|^2 \rangle \frac{d^2 q}{(2\pi)^2} \quad \text{if } r < \lambda_p,$$

$$C_r = \frac{1}{3} \int_{Q_r}^{Q_{\lambda_p}} q \langle |h(q)|^2 \rangle \frac{d^2 q}{(2\pi)^2} + \frac{7}{15\pi} \frac{\lambda_p}{r} \int_{Q_{\lambda_p}}^{Q_c} q \langle |h(q)|^2 \rangle \frac{d^2 q}{(2\pi)^2} \quad \text{if } r \geq \lambda_p, \quad (2)$$

$$F^T(T, r) \cong 1 + \frac{720}{\pi^2} \left[\left(\frac{K_B T r}{\hbar c} \right)^3 \frac{\zeta(3)}{2\pi} - \frac{45}{\pi^2} \left(\frac{K_B T r}{\hbar c} \right)^4 \right] \quad \text{if } K_B T r / \hbar c \leq 1/2,$$

$$F^T(T, r) \cong \left(\frac{K_B T r}{\hbar c} \right) \frac{\zeta(3)}{8\pi} - \frac{\pi^2}{720} \quad \text{if } K_B T r / \hbar c > 1/2, \quad (3)$$

and for the contact angle θ on a rough surface we have^{19,25}

$$\theta = \sqrt{2} \left((\theta_0 + \sqrt{2} \pi^{-1/2} \rho)^{-2} + \left\{ \cos^{-1} \left[\int_0^{+\infty} du (\sqrt{1+\rho^2 u}) e^{-u} \cos \theta_0 \right] \right\}^{-2} \right)^{-1/2}. \quad (4)$$

In Eqs. (2)–(4), $\langle |h(q)|^2 \rangle$ is the roughness spectrum, and $Q_c = \pi/a_0$ with a_0 a lower roughness cutoff of atomic dimensions. In Eq. (4) θ_0 is the theoretical contact angle on a flat surface which is given by Young's law.²⁶ The factor C_r in Eq. (2) arises from the roughness correction to the Casimir force taking into account finite conductivity corrections, which are based on power law approximations for wave vectors $q > 10^{-3}$.²² For shorter wave vectors, where the scattering is weak, the roughness spectrum approaches the asymptotic limit $\langle |h(q)|^2 \rangle \approx (2\pi)w^2 \xi^2$ for $q\xi \ll 1$ contributing less than the power law approximations as we approach the limit $q \rightarrow 0$. F^T is the temperature correction to the Casimir force as a multiplying factor.²³ Indeed, finite conductivity and temperature corrections may be treated independently and multiplied for theory estimations above the 1% accuracy level.²³ $\tilde{c}=c/\sqrt{\epsilon}$ is the velocity of light in the liquid between the plates, where we consider for simplicity constant the liquid dielectric function ϵ . $Q_{\lambda_p}=2\pi/\lambda_p$, $Q_r=2\pi/r$, $\zeta(3) \approx 1.202$ is the Riemann zeta function, and λ_p is the finite plasmon wavelength (e.g., ~ 100 nm for Al). $R_{Kel}=(\gamma U_m/RT) \times [|\log(P/P_{sat})|]^{-1}$ is the Kelvin condensation length, P/P_{sat} is the relative vapor pressure with P_{sat} the saturation pressure, γ is the surface tension, and U_m is the molar volume of the liquid. Indeed, capillary condensation is initiated for surface separation $r \geq d_0 [\approx 2R_{Kel} \cos \theta]$.²⁴

III. RESULTS AND DISCUSSION

The calculation of the pull-in voltage from Eq. (1) requires knowledge of the roughness spectrum $\langle |h(q)|^2 \rangle$. Indeed, a wide variety of thin film surfaces during nonequilibrium growth develops the so-called self-affine roughness for which $\langle |h(q)|^2 \rangle$ scales as²⁷ $\langle |h(q)|^2 \rangle \propto q^{-2-2H}$ if $q\xi \gg 1$ and $\langle |h(q)|^2 \rangle \propto \text{const}$ if $q\xi \ll 1$. This scaling behavior is satisfied by the analytic model²⁸

$$\langle |h(q)|^2 \rangle = 2\pi \frac{w^2 \xi^2}{(1+aq^2 \xi^2)^{1+H}}, \quad (5)$$

with $a=1/2H[1-(1+aQ_c^2 \xi^2)^{-H}]$ if $0 < H < 1$ and $a=1/2 \ln(1+aQ_c^2 \xi^2)$ if $H=0$. Small values of the roughness exponent $H(\sim 0)$ characterize jagged or irregular surfaces, while large values $H(\sim 1)$ surfaces with smooth hills and

valleys.²⁷ For other correlation models see also Refs. 27 and 29.

The Fourier transform of $\langle |h(0)|^2 \rangle$ yields the correlation function $g(r) = \langle [h(r) - h(0)]^2 \rangle$. The latter scales as $g(r) \propto r^{2H}$ for $r \ll \xi$ and yields $g(r)/r^2|_{r \rightarrow +\infty} \rightarrow 0$, if and only if $H < 1$, ensuring bounded roughness fluctuations (besides the restriction of a finite correlation length ξ). Equation (5) yields for the average local surface slope ρ the analytic form²¹

$$\rho = \sqrt{\int_0^{Q_c} q^2 \langle |h(q)|^2 \rangle d^2q / (2\pi)^2},$$

$$= (w/\sqrt{2}\xi a) \{ (1-H)^{-1} [(1+aQ_c^2\xi^2)^{1-H} - 1] - 2a \}^{1/2}. \quad (6)$$

The latter shows that the average local slope is proportional to the rms amplitude ($\rho \sim w$). The assumption of a Gaussian height distribution which yields the closed form $\int e^{-x} \sqrt{1+\rho^2 x} dx$ for the area integral is not restrictive within the weak roughness approximation ($\rho \ll 1$). This is because the dominant term up to second order in ρ yields $\sim 1 + (\rho^2/2)$ which can be obtained without any assumption about the height distribution.

In our calculations we have used $R_{\text{Kel}} = 1.6$ nm, which is the value for water at $T = 293$ K with $\gamma U_m / RT \approx 0.54$ nm, $\gamma = 73$ mJ/m², and relative humidity $P/P_{\text{sat}} = 0.5$.¹⁶ Note that in order to have $R_{\text{Kel}} \approx \lambda_p$ (≈ 100 nm), the required relative humidity is $P/P_{\text{sat}} \approx 0.99$, which is close to extreme humidity conditions for a microswitch to operate. Moreover, we used for the plasma wavelength the value $\lambda_p = 100$ nm and for simplicity $\varepsilon = 1$.

In former studies we investigated the variation of the contact angle θ on a rough surface as a function of the long wavelength ratio w/ξ and various roughness exponents H .²⁵ It was shown that for theoretical contact angles θ_0 lower than 90° , a weak maximum was observed for rather small roughness ratios w/ξ ($\ll 1$), while for larger ratios w/ξ the contact angle θ on a rough surface was a decreasing function of this ratio. The influence of the ratio w/ξ was more pronounced in the regime of theoretical contact angles $\theta_0 < 90^\circ$ and with increasing roughness exponent H the position of the maximum was moved at larger values of the ratio w/ξ .²⁵ Briefly, the contact angle on a rough surface appeared to have a relatively complex dependence on the roughness exponent H and the long wavelength ratio w/ξ .²⁵ The latter clearly necessitates a careful examination of the contact angle influence on pull-in characteristics of microswitches.

Figure 2 shows the direct dependence of the pull-in potential versus the roughness correlation length ξ for plates with dimensions $\Lambda = 5d$ (with $A_f = \Lambda^2$), $d = 80$ nm, $H = 0.9$, $u = 0.5$, $\varepsilon = 1$, $R_{\text{Kel}} = 1.6$ nm, $\lambda_p = 100$ nm, θ_0 as indicated in each graph, and various roughness amplitudes w as indicated.

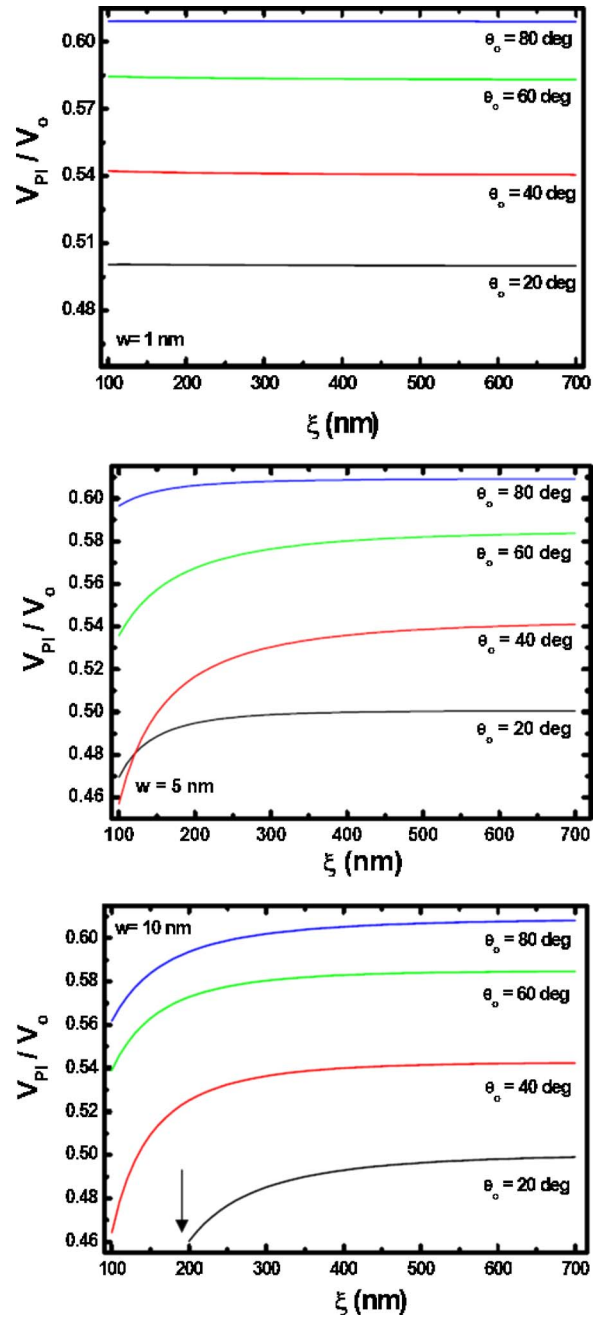


FIG. 2. (Color online) Pull-in voltage ratio vs lateral roughness correlation length ξ for plates with dimensions $\Lambda = 5d$ (with $A_f = \Lambda^2$), $d = 80$ nm, $H = 0.9$, $u = 0.5$, $\varepsilon = 1$, $R_{\text{Kel}} = 1.6$ nm, $\lambda_p = 100$ nm, θ_0 as indicated in each graph, and various roughness amplitudes w as indicated.

Similarly to Fig. 2, we plot in Fig. 3 the pull-in potentials for two different roughness exponents H and different contact angles θ_0 . With decreasing exponent H the pull-in potential shows a significant steep increase with increasing correlation length when the latter remains significantly small ($< 2\lambda_p$). This behavior persists even with relatively large contact angles θ_0 . This is because, with increasing surface roughness it also increases the local surface slope ρ , and thus it decreases the actual contact angle θ , leading to larger capillary forces, and as a result to a lower pull-in potential due to the presence of the $\sim \cos^2(\theta)$ term in Eq. (1).

For sufficiently small correlation lengths, as it is shown

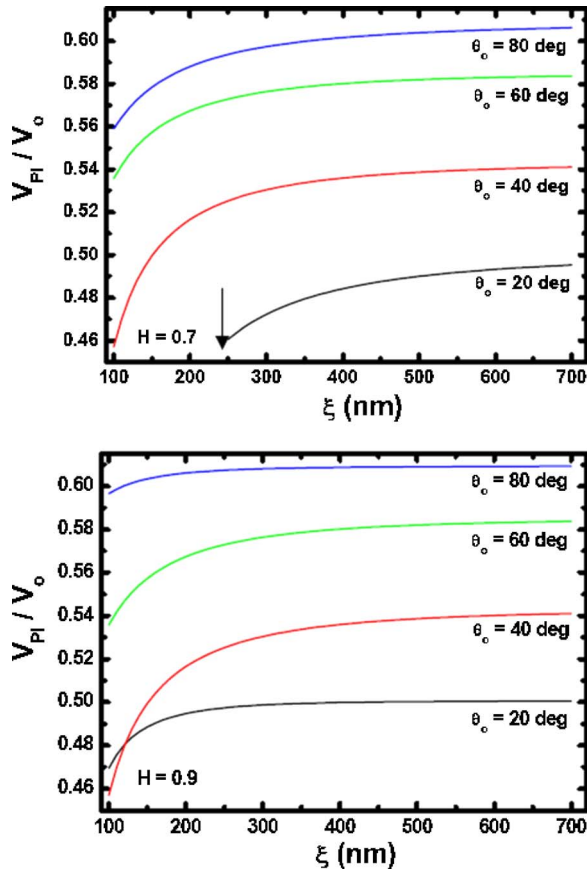


FIG. 3. (Color online) Pull-in voltage ratio vs lateral roughness correlation length ξ for plates with dimensions $\Lambda=5d$ (with $A_f=\Lambda^2$), $d=80$ nm, $w=5$ nm, H as indicated, $u=0.5$, $\epsilon=1$, $R_{\text{Kel}}=1.6$ nm, $\lambda_p=100$ nm, and θ_0 as indicated in each graph.

by the arrows in Figs. 2 and 3, the roughness contribution was significant enough to give a negative difference in the square root of Eq. (1). The latter represents alternatively an instantaneous collapse of the switch beyond which any mechanical movement is fully disrupted by the capillary contribution. Moreover, as Fig. 4 shows with decreasing correlation length ξ (or equivalently increasing surface roughness

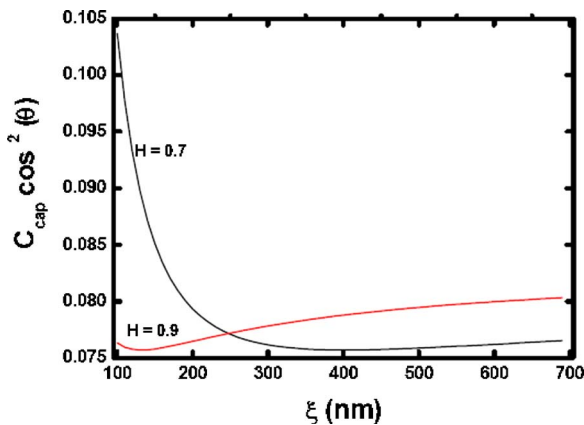


FIG. 4. (Color online) Plot of the capillary contribution $C_{\text{cap}} \cos^2(\theta)$ [$C_{\text{cap}} = (8\gamma R_{\text{Kel}}/\epsilon V_0^2)$] on the pull-in voltage in Eq. (1) vs lateral roughness correlation length ξ for plates with dimensions $\Lambda=5d$ (with $A_f=\Lambda^2$), $d=80$ nm, $w=5$ nm, $\theta_0=40^\circ$, H as indicated, $u=0.5$, $\epsilon=1$, $R_{\text{Kel}}=1.6$ nm, $\lambda_p=100$ nm, and θ_0 as indicated in each graph.

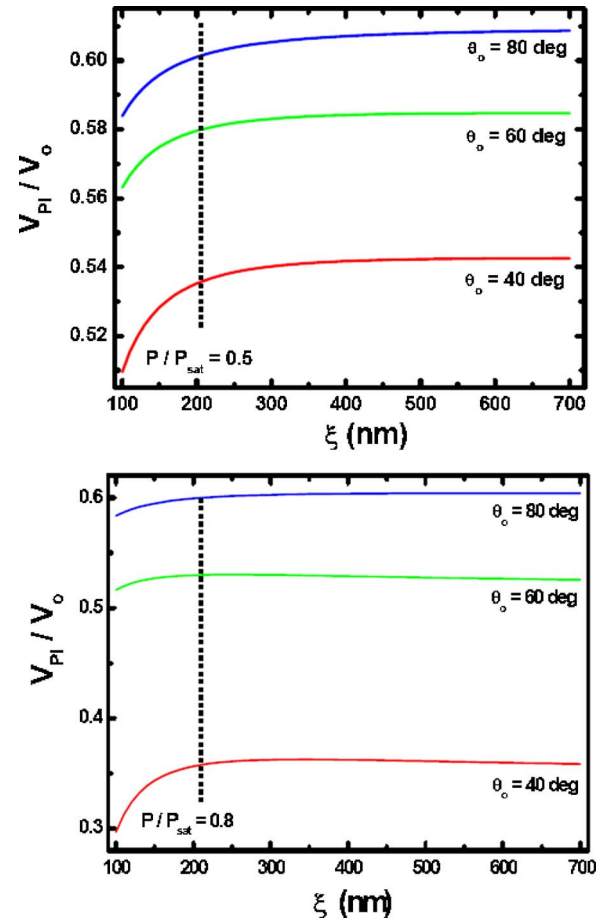


FIG. 5. (Color online) Pull-in voltage ratio vs lateral roughness correlation length ξ for plates with dimensions $\Lambda=5d$ (with $A_f=\Lambda^2$), $d=80$ nm, $w=5$ nm, $H=0.8$, $u=0.5$, $\epsilon=1$, $R_{\text{Kel}}=1.6$ nm, $\lambda_p=100$ nm, two different values of the relative humidity P/P_{sat} , and θ_0 as indicated in each graph.

for fixed roughness amplitude w), the capillary term in Eq. (1), $(8\gamma R_{\text{Kel}}/\epsilon V_0^2)\cos^2(\theta)$, shows a weak minimum and a steep increase with decreasing correlation length ξ and roughness exponent H . This behavior of the capillary term explains the corresponding decrement of the pull-in voltage with decreasing correlation length ξ and decreasing roughness exponent H in Figs. 2 and 3.

Finally, as Fig. 5 indicates with increasing relative humidity P/P_{sat} , the sensitivity of the pull-in voltage at small correlation lengths ($\xi < 2\lambda_p$) attenuates significantly with increasing contact angle θ_0 . This is shown by the dashed line in the schematics of Fig. 4 for two different values of the relative humidity. This is because the capillary contribution in Eq. (1) is proportional to an increasing Kelvin condensation length R_{Kel} with increasing relative humidity. As a result it leads to a larger capillary term and a lower influence of the terms that originate only from the contributions of electrostatic and Casimir forces.

IV. CONCLUSIONS

The presence of capillary condensation between microswitch plates lowers the effective pull-in voltage derived by the application of an electric potential in a manner that depends significantly on the contact angle of the capillary

meniscus. It was shown that surface roughening has stronger influence on the pull-in potential for relatively small contact angles, with respect to that of a flat surface, when capillary condensation takes place. Indeed, with decreasing long wavelength roughness ratio so that $w/\xi \ll 1$ (corresponding to weak surface roughness), the pull-in voltage increases with increasing contact angle θ_0 . However, with increasing ratio w/ξ , the pull-in voltage shows a sensitive increment with increasing correlation length ξ , which becomes steeper with decreasing contact angle θ_0 . Similarly with decreasing roughness exponent H , which corresponds to rougher surfaces at short length scales ($< \xi$), the pull-in potential shows a significant steep increase with increasing correlation length as long as it remains sufficiently small. In addition, with increasing relative humidity, which leads to larger Kelvin condensation lengths, the sensitivity of the pull-in voltage at small correlation lengths attenuates also significantly with increasing contact angle θ_0 . Future studies will address in more accurate manner the influence of the liquid dielectric properties through the Casimir force. In addition, dynamic considerations will be implemented in calculating the influence of Casimir and capillary force effects to the pull-in velocity in order to shed light on their relative contribution in plate motion, since the inclusion of both forces has to be taken into account if the device operates in a wet environment.

¹H. J. De Los Santos, Proc. IEEE **91**, 1907 (2003); K. L. Ekinci and M. L. Roukes, Rev. Sci. Instrum. **76**, 061101 (2005).

²S. Akita *et al.*, Appl. Phys. Lett. **79**, 1691 (2001).

³P. M. Osterberg, Ph.D. dissertation, Massachusetts Institute of Technology, 1995.

⁴O. Bochobza-Degani and Y. Nemirowsky, Sens. Actuators, A **97-98**, 569 (2002).

⁵O. Bochobza-Degani, E. Socher, and Y. Nemirowsky, Sens. Actuators, A **97**, 563 (2002).

⁶L. X. Zhang, J. W. Zhang, Y.-P. Zhao, and T. X. Yu, Int. J. Nonlinear Sci. Numer. Simul. **3**, 353 (2002).

⁷L. X. Zhang and Y.-P. Zhao, Microsyst. Technol. **9**, 420 (2003).

⁸L. J. Hornbeck, U.S. Patent No. 5,061,049 (October 29 1991).

⁹E. Buks and M. L. Roukes, Europhys. Lett. **54**, 220 (2001).

¹⁰M. Dequesnes, S. V. Rotkin, and N. R. Aluru, Nanotechnology **13**, 120 (2002).

¹¹S. V. Rotkin, Proc.-Electrochem. Soc. **6**, 90 (2002).

¹²W. H. Lin and Y.-P. Zhao, Chin. Phys. Lett. **20**, 2070 (2003).

¹³W. H. Lin and Y.-P. Zhao, Chaos, Solitons Fractals **23**, 1777 (2005).

¹⁴R. Maboudian and R. T. Howe, J. Vac. Sci. Technol. B **15**, 1 (1997).

¹⁵H. B. G. Casimir, Proc. K. Ned. Akad. Wet. **51**, 793 (1948).

¹⁶J. N. Israelachvili, *Intermolecular and Surface Forces* (Academic, London, 1992); A. W. Adamson, *Physical Chemistry of Surfaces*, 5th ed. (Wiley, New York, 1990).

¹⁷M. Kardar and R. Golestanian, Rev. Mod. Phys. **71**, 1233 (1999); M. Bordag, U. Mohideen, and V. M. Mostepanenko, Phys. Rep. **353**, 1 (2001); V. M. Mostepanenko and N. N. Trunov, *The Casimir Effect and its Applications* (Clarendon, Oxford, 1997).

¹⁸G. Palasantzas and J. Th. M. De Hosson, Phys. Rev. B **72**, 115426 (2005); Phys. Rev. B **72**, 121409 (2005); G. Palasantzas and J. Th. M. De Hosson Surf. Sci. **600**, 1450 (2006).

¹⁹G. Palasantzas, J. Appl. Phys. **100**, 054503 (2006).

²⁰B. N. J. Persson and E. J. Tosatti, J. Chem. Phys. **115**, 5597 (2001).

²¹G. Palasantzas, Phys. Rev. E **56**, 1254 (1997).

²²P. A. Maia Neto, A. Lambrecht, and S. Reynaud, Phys. Rev. A **72**, 012115 (2005).

²³C. Genet, A. Lambrecht, and S. Reynaud, Phys. Rev. A **62**, 012110 (2000); C. L. Klimchitskaya and V. M. Mostepanenko, *ibid.* **63**, 062108 (2001); M. Bordag, U. Mohideen, and V. M. Mostepanenko, Phys. Rep. **353**, 1 (2001).

²⁴P. G. de Gennes, Rev. Mod. Phys. **57**, 827 (1984); L. Leger and J. F. Joanny, Rep. Prog. Phys. **55**, 431 (1992).

²⁵G. Palasantzas and J. Th. M. De Hosson, Acta Mater. **49**, 3533 (2001).

²⁶S. Mason, *Wetting Spreading and Adhesion*, edited by J. F. Panday (Academic, New York, 1978).

²⁷P. Meakin, Phys. Rep. **235**, 1991 (1994); J. Krim and G. Palasantzas, Int. J. Mod. Phys. B **9**, 599 (1995).

²⁸G. Palasantzas, Phys. Rev. B **48**, 14472 (1993); **49**, 5785 (1994).

²⁹S. K. Sinha, E. B. Sirota, S. Garoff, and H. B. Stanley, Phys. Rev. B **38**, 2297 (1988); H. N. Yang and T. M. Lu, Phys. Rev. E **51**, 2479 (1995); Y. P. Zhao, G. C. Wang, and T. M. Lu, Phys. Rev. B **55**, 13938 (1997); G. Palasantzas and J. Krim, *ibid.* **48**, 2873 (1993).